Lecture Notes in Mechanical Engineering

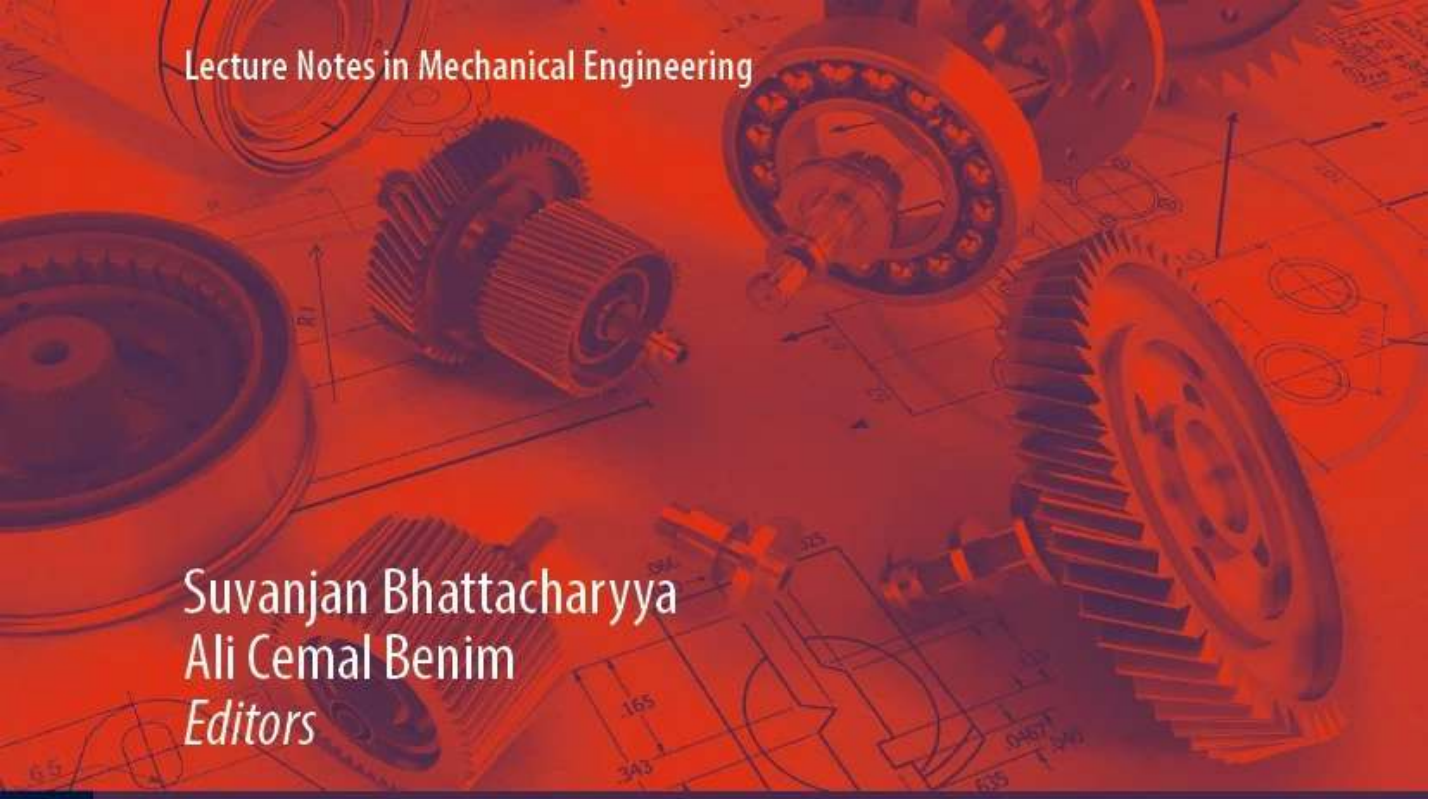

Suvanjan Bhattacharyya
Ali Cemal Benim
Editors

Fluid Mechanics and Fluid Power (Vol. 2)

Select Proceedings of FMFP 2021

Springer

Proceedings of the 48th National Conference on Fluid Mechanics and Fluid Power (FMFP)
December 27-29, 2021, BITS Pilani, Pilani Campus, RJ, India.

FMFP2021-10-136

Numerical Analysis of Open-Water Propeller Performance and Submarine Hull Drag

Pritam Ghosh[1], Pranibesh Mandal[2]

[1]Department of Mechanical Engineering, Heritage Institute of Technology, Kolkata-700107, India
[2]Department of Mechanical Engineering, Jadavpur University, Kolkata-700032, India

ABSTRACT

The selection of appropriate propeller size meets the need of a submarine to move forward with the desired velocity against hull drag. In the present study, the Open-water behavior of a B-series four-bladed propeller and hull drag of a submarine with a realistic geometry have been studied through numerical simulation by using the ANSYS-Fluent software platform. The rotation of the propeller has been given by frame motion and the Shear Stress Transport (SST) k-ω model has been used for turbulence flow modeling. The grid independence test has also been performed at the onset. The propeller performance coefficients and submarine hull drag have been obtained by varying flow velocity. This result has helped in predicting the maximum thrust of the propeller and maximum velocity of the submarine. For validation purposes, the results of propeller coefficients obtained from numerical simulation have been compared with experimental data of existing literature and found good acceptance.

Keywords: B-series Propeller, Grid Independency, Open-water Performance, Propeller thrust, Submarine hull drag, Turbulence model.

1. INTRODUCTION

In marine propulsion, the widely used propeller and its design play a very crucial role. Moreover, from the point of view of the power estimation, the submarine's hull-propeller interaction has great importance. The main objective of designing a propeller is to provide maximum thrust and minimum torque for the optimum rotational speed. Besides, achieving the maximum efficiency, low noise and lighter weight also fall under the shade of propeller design. Until and unless these designed propellers are not tested through experiments, the actual performance of these propellers cannot be found out. However, such experiments are not only too expensive and time taking, but also assessment of such propeller behind hull where the highly disturbed wake zone exists is really a challenging job [1]. Thanks to the rapid development and advancement of computational fluid dynamics (CFD) technology it is possible to conduct such studies numerically in a simulation frame and to achieve very close prediction of actual propeller performance in real-time. Basically in an open-water test, the propeller is tested in towing tank without the hull. Here, the performance characteristic attributes viz. thrust and torque coefficients as well as the efficiency with advance ratio, are measured as the efficiency of the propulsion system is greatly dependent on these performance attributes.

2. LITERATURE REVIEW AND OBJECTIVE

In 2017, Delen et al. [2] evaluated the power and resistance of a submarine (DARPA SUBOFF) using both numerical analysis and empirical method. In their research, the open-water analysis of propeller was done numerically and finally validated with experimental data. Besides, the self-propulsion of the vehicle was studied using different velocities. They also applied the Actuator Disc Theory in self-propulsion tests with CFD for making the analysis robust. Investigation on resistance characteristic of a DARPA-SUBOFF submarine was done by Budak and Beji [3]. In this study taking the DARPA-SUBOFF submarine as a base model, nine geometric variant models were developed by combining three slightly different bow and three different stern forms with each other. Analysis of these newly developed submarine model had been done using commercial software ANSYS-FLUENT where SST k-ω model was used for computation. Since power is limited to any underwater submarine, minimization of hull drag could provide a longer dive span to the submarine. While designing any submarine hull, one should focus on various hydrodynamic parameters which play very significant role in submarine motion during submerged condition. Drag of submarine is one of them. In 2018 Ghosh and Mandal [4] have worked on pressure and shear stress distribution on an autonomous underwater vehicle's hull. A 3D submarine hull in the simulation frame has been used to conduct the study using ANSYS-FLUENT software and analyze the distribution of pressure and shear stress distribution over the external hull of the submarine. Taskar et al. [5] have worked on propulsion system of a ship to investigate the propulsion at different wave conditions. To do so they used an inertial shaft model and applied a methodology for estimation of wake in waves. From their study it has been observed that there is a drop in propulsion performance when they considered the engine propulsion dynamics, wake variations and other losses. For power performance of any submarine, hull-propeller interaction plays an important role. In 2014, Nan and Sheng-li [6] studied on five bladed propeller having a high-skew of a submarine

S. Bhattacharyya and A. C. Benim (eds.), *Fluid Mechanics and Fluid Power (Vol. 2)*,
Lecture Notes in Mechanical Engineering, https://doi.org/10.1007/978-981-19-6970-6_30

model in submerged and near surface conditions using computational method. Volume of Fluid (VOF) method has been implemented and sliding mesh technique has been used for giving rotation to the propeller. They compared the numerical solution of various propeller performance attributes viz. thrust, torque etc. with experimental data and found good agreement.

Recently Ghosh and Mandal [7] have studied on an innovative underwater vehicle which has four ballast tanks for controlling of depth, roll and pitch motion. The main objective of their study was to eliminate some of the control surfaces by placing the ballast tanks innovatively. In the present study a similar type of submarine model having a realistic geometry has been used. For this submarine a suitable propeller is required to provide the forward motion to the submarine against hull drag. Based on this scope, the objectives of this present study are drawn as follows:

- To choose a suitable size of propeller relevant to submarine size.
- To design the propeller based on its chosen size.
- To measure the performance of the designed propeller.
- To measure the submarine drag force at different submarine speeds.
- To compare the propeller thrust with submarine drag force.

3. GEOMETRY AND NUMERICAL METHODOLOGY

In this study an innovative and realistic submarine model [7] has been used. This model submarine is of 1 m in overall hull length, 0.2 m in maximum width and 0.16 m in height. It consists of control surfaces on rear and four ballast tanks inside. SolidWorks software has been used for constructing this model which is shown in Fig. 1. The propeller model used is a four bladed, right-hand, skewed B-series propeller having outer diameter (D) of 0.16 m. and area ratio (A_E/A_O) equal to 0.8. Other details of the propeller geometry is given in Table 1 along with a modified modeled propeller which has been drawn with the help of AutoCAD and SolidWorks software as shown in Fig. 2, Fig. 3 and in Fig. 4.

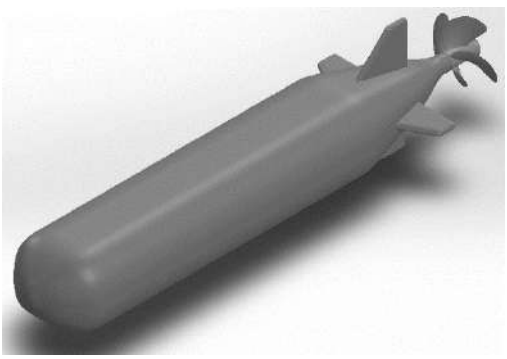

Figure 1: Geometrical model of the submarine

Figure 2: Geometrical model of propeller (side view)

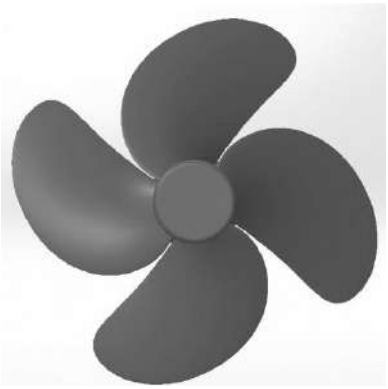

Figure 3: geometrical model of propeller (front view)

Table 1: Important propeller parameters

r/R	Pitch-diameter ratio (*P/D*)	Skew (degree)	Chord-diameter ratio (*c/D*) in %	Blade thickness ratio (*t/D*) in %
1	1	32.00	0.48	0.24
0.95	1	26.89	40.09	0.86
0.90	1	21.62	53.07	1.23
0.80	1	10.98	66.98	1.98
0.70	1	2.79	71.82	2.73
0.60	1	-2.96	71.44	3.49
0.50	1	-6.70	68.00	4.24
0.40	1	-8.85	62.77	4.99
0.30	1	-9.99	56.01	5.74
0.20	1	-9.80	47.96	6.49

Paper ID: ICERTSD 216

Computational Study of Shock Diffraction over Rounded Corners

Debiprasad Banerjee* and Pabitra Halder

*Mechanical Engineering Department, Heritage Institute of Technology, Kolkata-700107, West Bengal, India

debiprasad.banerjee@heritageit.edu

Abstract

Shock wave motion is important in many areas of engineering like blast wave modeling, medical applications, aeronautical design, etc. Aerodynamic testing is increasingly dominated by numerical research where shock wave diffraction is one of the fastest transient fluid flow processes. Mostly, previous works emphasized on sharp or abrupt changes in geometry which causes immediate flow separation. In present study, round corners are investigated and the intricate flow features are summarized. Numerical simulations are performed using Finite Volume Method. The rounded geometry requires laminar viscosity model due to continuous changes of the orientation. The unsteady flow field is designed to have an understanding appropriate to the actual test case under consideration. The shock diffraction process, shear layer, vortex generation, secondary and tertiary waves are clearly investigated.

Keywords: Shock diffraction, flow separation, laminar viscosity, unsteady flow, Shear layer, vortex generation.

**Corresponding author address and email*

Doctoral Symposium on Human Centered Computing

Human 2023: **Intelligent Human Centered Computing**, pp 74–85

Job Recommendation a Hybrid Approach Using Text Processing

Dipanwita Saha, Dinabandhu Bhandari & Gunjan Mukherjee

Conference paper | First Online: 15 June 2023

Part of the Springer Tracts in Human-Centered Computing book series (STHCC)

Abstract

This work is an attempt to collate the data and discover the foremost relevant candidate-job association mapping concurring with the skills, interests, and preferences of a user and to provide a possible job opportunity as an efficient solution. Several personalized content-based and case-based approaches are considered in this regard. The investigation involves several feature-based item representation methods along with feature-

weighted schemes. A comparative evaluation of the distinctive perspective is performed utilizing Kaggle data respiratory. The investigation of this study has shown that job transitions can be successfully predicted. The delicacy of the model can be evaluated based on various algorithms of machine learning such as Naïve Bayes, Logistic regression, support vector machine, random forest, K-nearest neighbors, and multilayer perceptron. In this work, the hybrid recommender framework is created to analyze the further investigation in advance to make an identification of the region of opportunity for the prediction of a suitable job. To get the most expected outcome optimization techniques has applied and after utilization of various machine learning algorithms on hybrid approaches, the classifier of Random Forest gives better results. By this examination, the system of job recommendation can give proper assistance to job searchers improving accuracy and scalability.

Keywords

Natural Language Processing

Machine Learning **Random Forest**

Hybrid model **Optimization**

References

1. Anand, P.B., Nath, R.: Content-Based Recommender Systems. In: Recommender System with Machine Learning and Artificial Intelligence: Practical Tools and Applications in

Medical, Agricultural and Other Industries, pp. 165–195 (2020)

2. Amara, S., Raja Subramanian, R.: Collaborating personalized recommender system and content-based recommender system using TextCorpus. In: 2020 6th International Conference on Advanced Computing and Communication Systems (ICACCS). IEEE (2020)

3. Ameen, A.: Knowledge based recommendation system in semantic web-a survey. Int. J. Comput. Appl. **182**(43), 20–25 (2019)

4. Gugnani, A., Misra, H.: Implicit skills extraction using document embedding and its use in job recommendation. In: Proceedings of the AAAI Conference on Artificial Intelligence, vol. 34, no. 08 (2020)

5. Yadalam, T.V., et al.: Career recommendation systems using content based filtering. In: 2020 5th International Conference on Communication and Electronics Systems (ICCES). IEEE (2020)

6. Sun, Y., et al.: Cost-effective and interpretable job skill recommendation with deep reinforcement learning. In: Proceedings of the Web Conference 2021 (2021)

7. Çak, M., Öğüdücü, Ş, Tugay, R.: A deep hybrid model for recommendation systems. In: Alviano, M., Greco, G., Scarcello, F. (eds.) AI*IA 2019. LNCS (LNAI), vol. 11946, pp. 321–335. Springer, Cham (2019). https://doi.org/10.1007/978-3-030-35166-3_23

8. Valverde-Rebaza, J.C., et al.: Job Recommendation Based on Job Seeker Skills: An Empirical Study. Text2Story@ ECIR (2018)

9. Bansal, S., Srivastava, A., Arora, A.: Topic modeling driven content based jobs recommendation engine for recruitment industry. Procedia Comput. Sci. **122**, 865–872 (2017)

10. Desai, V., et al.: Implementation of an automated job recommendation system based on candidate profiles. Int. Res. J. Eng. Technol. **4**(5), 1018–1021 (2017)

11. Tran, M.-L., et al.: A comparison study for job recommendation. In: 2017 International

Conference on Information and Communications (ICIC). IEEE (2017)

12. Guo, X., Jerbi, H., O'Mahony, M.P.: An analysis framework for content-based job recommendation. In: 22nd International Conference on Case-Based Reasoning (ICCBR), Cork, Ireland, 29 September–01 October 2014 (2014)

13. Al-Otaibi, S.T., Ykhlef, M.: Job recommendation systems for enhancing e-recruitment process. In: Proceedings of the International Conference on Information and Knowledge Engineering (IKE). The Steering Committee of The World Congress in Computer Science, Computer Engineering and Applied Computing (WorldComp) (2012)

14. Zhao, J., et al.: Embedding-based recommender system for job to candidate matching on scale. arXiv preprint arXiv:2107.00221 (2021)

15. Islam, R., et al.: Debiasing career recommendations with neural fair collaborative filtering. In: Proceedings of the Web Conference 2021 (2021)

16. Zheng, Y., Pu, A.: Utility-based multi-stakeholder recommendations by multi-objective optimization. In: 2018 IEEE/WIC/ACM International Conference on Web Intelligence (WI). IEEE (2018)

17. Mhamdi, D., et al.: Job recommendation based on job profile clustering and job seeker behavior. Procedia Comput. Sci. **175**, 695–699 (2020)

18. Heggo, I.A., Abdelbaki, N.: Data-driven information filtering framework for dynamically hybrid job recommendation. In: Gherabi, N., Kacprzyk, J. (eds.) Intelligent Systems in Big Data, Semantic Web and Machine Learning. AISC, vol. 1344, pp. 23–49. Springer, Cham (2021). https://doi.org/10.1007/978-3-030-72588-4_3

Author information

Authors and Affiliations

Department of Computer Science and Engineering, Abacus Institute of Engineering and Management, Hooghly, West Bengal, India
Dipanwita Saha

Department of Computer Science and Engineering, Heritage Institute of Technology, Kolkata, West Bengal, India
Dinabandhu Bhandari

Department of Computational Science, Brainware University, Kolkata, West Bengal, India

Gunjan Mukherjee

Corresponding author

Correspondence to Dipanwita Saha .

Editor information

Editors and Affiliations

Algebra University College, Zagreb, Croatia

Siddhartha Bhattacharyya

Department of Computer Science and Engineering (AI & ML), Bengal Institute of Technology, Kolkata, India

Jyoti Sekhar Banerjee

Department of Computer Science and Engineering, Maulana Abul Kalam Azad University of Technology, Kolkata, West Bengal, India

Debashis De

Department of Computer Science, Nottingham Trent University, Nottingham, UK

Mufti Mahmud

Rights and permissions

Copyright information

About this paper

Cite this paper

Saha, D., Bhandari, D., Mukherjee, G. (2023). Job Recommendation a Hybrid Approach Using Text Processing. In: Bhattacharyya, S., Banerjee, J.S., De, D., Mahmud, M. (eds) Intelligent Human Centered Computing. Human 2023. Springer Tracts in Human-Centered Computing. Springer, Singapore. https://doi.org/10.1007/978-981-99-3478-2_8

.RIS .ENW .BIB

DOI	Published	Publisher Name
https://doi.org/10.1007/978-981-99-3478-2_8	15 June 2023	Springer, Singapore

Print ISBN	Online ISBN	eBook Packages
978-981-99-3477-5	978-981-99-3478-2	Intelligent Technologies and Robotics Intelligent Technologies and Robotics (R0)

INTERNATIONAL JOURNAL OF MICROWAVE AND OPTICAL TECHNOLOGY,
VOL.18, NO.3, MAY 2023

Metamaterial Embedded Multi-Notched Ultra-Wideband Monopole Antenna

Susobhan Ray[1], Chittajit Sarkar[2]*, Khushi Banerjee[3], Mahuya Maity[4], Ipsita Ghosh[5], Sayantani Datta[6]

[1,5]Swami Vivekananda Institute of Science and Technology ,[2,3]Asansol Engineering College,
[4]Calcutta Institute of Technology ,
[6]Heritage Institute of Technology
*E-mail: chittajit.ece@aecwb.edu.in

***Abstract*- Proposal and comprehension of spur line embedded frequency notched Ultrawideband antenna is projected in this paper. The performance of the antenna is enhanced by using square shaped metamaterial. Quarter-wavelength long spur line (lines) on the feeding microstrip line of UWB antenna backs a notch-filtering action to provide single/double/triple notch (notches) within the UWB spectrum of the antenna. The planned method is very simple and radiator independent. The conventional monopole antenna is loaded with square shaped metasurface (MS) to enhance the performance of the antenna. With and without metamaterial loaded single, double and triple spur-line embedded microstrip fed circular monopole antennas are separately designed, fabricated and measured. All the deliberate models are fabricated and considered for measurement of impedance and radiation characteristics .Measured results show very good consistency with that of results obtained from full wave simulation.**

***Index Terms*- Metamaterial, Notched antenna, Spur line filter, UWB Antenna.**

I. INTRODUCTION

Research on UWB technology remained quiescent for quite a few decades due to various issues like dispersion, power restriction, short range, etc. However, with the ever growing demand of high speed and high data rate communication, created a new landmark in wireless industry in 2002 when a special band of 3.1-10.6 GHz was assigned for UWB communication by FCC with proscribed power level [2]. However the band conjoining of this approved UWB spectrum with different narrow band services, such as Wi-MAX(3.3-3.7GHz) ,WLAN(5.170-5.815 GHz) and 7.25-7.75 GHz X-band satellite downlink etc. forced extra bondage of impeding spread over these narrow band services. Copious UWB researches/groups have conveyed this narrow band interference elimination method over the last decades. These interference lessening practice can be mostly categorized as : (a) launching different shaped slots on the radiator/ or in the feed region,(b) using parasitic resonator around/beneath the radiator [3]-[8].(c) blending of (i) and (ii).The major flaws in attaining the frequency notch by these technique are i) conciliation in radiation performance of the antenna in the expected frequency band, ii) designs are not simply /readily scalable to the new desired frequency, iii) the designs are extremely precise to antenna geometry .An alternative method of frequency notched UWB antenna scheme by presenting a pair of split ring resonator in the feed region of the CPW fed UWB monopole antenna presented in [9]. Loading of such SRR in the aperture of the horn antenna [10] has been introduced to design frequency notched horn antenna. Two dissimilar methods of SRR stacking have been recently projected [10] to plan antipodal tapered slot antenna with assimilated frequency notched features.

In this paper, a quarter wave length spur line implanted on the feeding microstrip section of the antenna is anticipated. The quarter wave length long spur line efficiently turns as parallel resonant circuit [11]-[17], compliant with the band rejection possessions at its resonant

frequency. Dual/triple band-notched enactments were achieved by using multiple spur lines of changing length.Key losses in the form of 'surface waves' in antenna have been considerably reduced as illuminated in [18]. The modification of RF signals with square shaped metamaterials placed on the antenna radiator plane is the central appeal of this paper. Thus in this proposal, the design of filtering section, square shaped meta-surfaces and the radiator are entirely independent.

The originality of the proposal is that due to placement of periodic metasurface the attainable maximum realized gain is 6.45 dBi that is little bit higher than the conventional frequency notched Monopole antenna 5.47dBi. The paper is

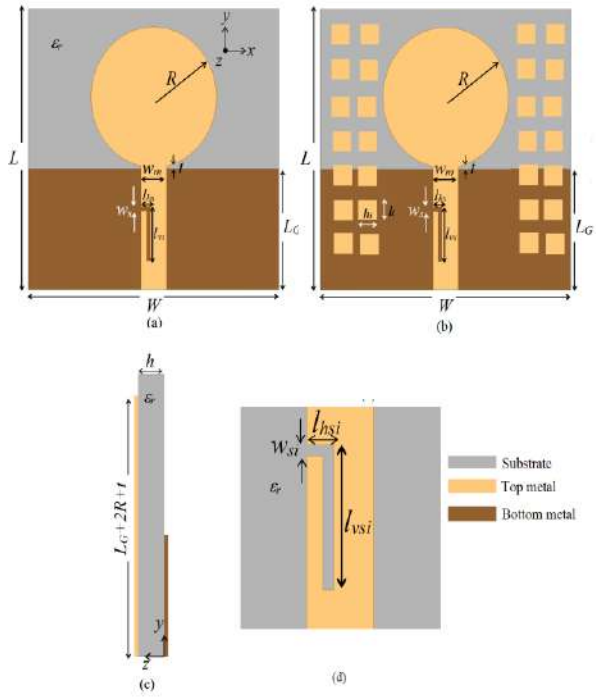

Fig.1. Schematic of a microstrip-fed printed circular MPA loaded with spur line resonator (a) Top view of monopole antenna with spur-line on feed-section of the antenna. (b)Top view of monopole antenna loaded with square shape metamaterial (c) Side view showing the printed monopole separated by h from the ground plane on the other side of the substrate. (c) Enlarged view of the spur line resonator printed on the microstrip-line

covered as follows: Section-II deliberates the design steps of the projected frequency notched UWB antenna. Design and apprehension of the notch-filters along with validation using EM simulation and S-parameters measurements of the fabricated prototype is conversed in Section -III. Section-IV deals with the complete impedance and radiation characteristics measurements of fabricated antenna prototype. The paper is concluded in Section –V.

II. ANTENNA DESIGN

Figure 1(a) and (b) shows the diagram of the projected spur line embedded and metamaterial loaded microstrip fed frequency notched UWB Monopole antenna. The central UWB radiator is a circular monopole of radius R fed by 50-ohm microstrip line of width Wm and length (LG+t) . Fig 1(a), shows a quarter wave length spur line of length l_{vs} and width w_s, housed on the feeding microstrip line of the MPA. Figure 1(c) shows the exaggerated view of the i-th spur line, where i ranges from 1 to 3, for single, dual and triple notched operation of the proposed UWB antenna. The stand alone circular MPA without any spur-line on the feeding microstrip, acts as the basic UWB radiator [19]-[20]. Embedding a quarter wave spur line of length l_{vsi} yields a notch frequency f_n given by,

$$l_{vs} = \frac{\lambda_n}{4} = \frac{c}{4 f_n \sqrt{\varepsilon_{reff}}} \quad (1)$$

$$f_n = \frac{c}{4\sqrt{\varepsilon_{reff}}\, l_{vs}} \quad (2)$$

Where ε_{reff} is the effective dielectric constant obtained from well-known empirical equation [21] .The equivalent circuit of the proposed antenna is shown in fig.2.

Three set of prototype antennas are fabricated on Taconic substrate having ε_r = 2.33, tan δ = 0.0012 and thickness h =1.575 mm. The detail design parameter of the planned model antenna are shown in Table I.

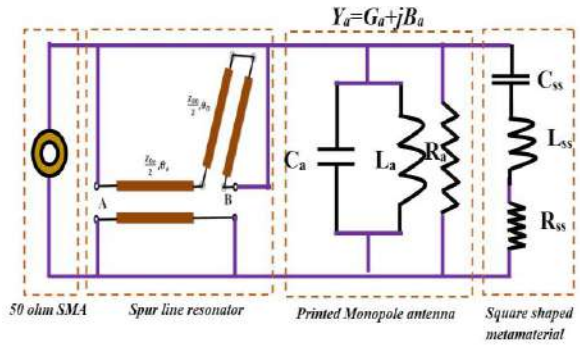

Fig.2 Equivalent circuit of square shaped metamaterial loaded monopole antenna embedded with Spurline.

The radiation patch of the printed monopole is represented by a lossy shunt resonator composed of Ra, L_a and C_a. Where, R_a is equivalent to the radiation resistance of the printed monopole antenna. The admittance of the 'traditional' printed monopole antenna is , $Y_a = G_a + jB_a$ Where, G_a and B_a is the real part and imaginary part of admittance Y_a, respectively.

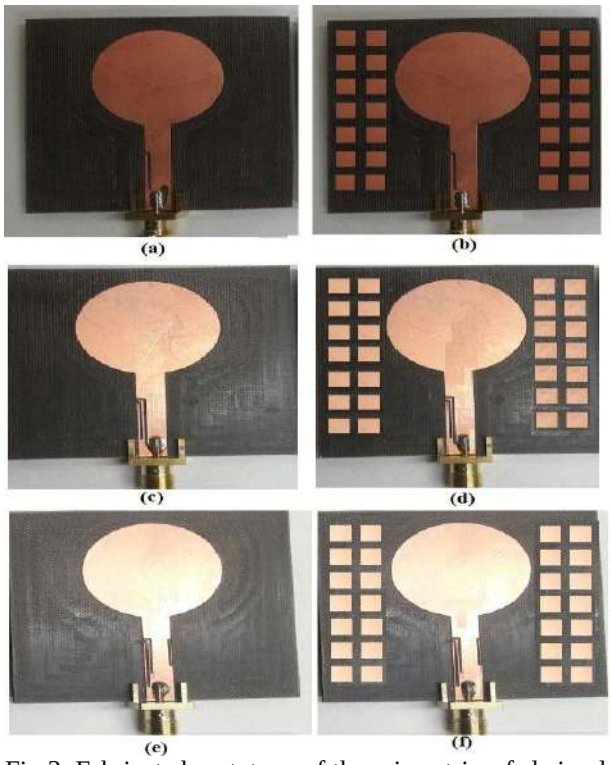

Fig.3. Fabricated prototype of the microstrip fed circular monopole antenna loaded with spur-line filter sections. Top View of (a) single spur without metamaterial, (b) single spur with metamaterial (c) double spur without metamaterial, (d) double spur with metamaterial (e) triple spur without metamaterial, (f) triple spur with metamaterial .

The square shaped metamaterial impedance, consisting of series resonators,

$$Z_{ss}=R_{ss}+jw\ L_{ss}+1/jwC_{ss}$$

Where L_{ss} is the inductance corresponding to the length (h_i=l_i) of the square shaped metamaterial and C_{ss} is the capacitance between two adjacent unit cells. R_{ss} is the resistance of the top copper patch with finite conductivity.

The spur line equivalent circuits consists of transmission line with characteristics impedance $Z_{oe}/2$ and electrical length θ_e connected in series with characteristics impedance $Z_{o0}/2$ and electrical length θ_o [13]-[14].

III.MEASUREMENT OF NOTCHED METAMATERIAL LOADED ANTENNA

Here, the design of antenna and filtering section are totally independent as the filter is housed in the feeding microstrip with no direct bang on radiating part of the antenna. Figure 3 shows the fabricated model of the projected single, dual and triple spur line integrated antenna loaded with square shaped metamaterial. The antennas are planned and simulated in a commercial EM simulator [22]. All the fabricated models are methodically experimented for impedance and radiation characteristics measurements. A fully calibrated near field anechoic chamber was used to measure radiation pattern of all the fabricated models.

A. Single Notched Metamaterial Loaded Antenna

Figure 3(a) shows a fabricated prototype of a single notched without metamaterial UWB antenna. Figure 3(b) shows a fabricated prototype of a single notched metamaterial loaded UWB antenna. As discovered from the Fig. 1, single notched UWB response can be achieved by a single spur line embedded on the feeding microstrip of the circular MPA . Fig.4 shows the simulated and measured S_{11} versus frequency plot of the single spur-line embedded MPA with and without metamaterial. From the plot it is clear that a measured notch frequency at 5.63 GHz against 5.53 GHz for simulated notch was obtained due to the presence of the quarter wave length single spur line. Fig. 5 shows the measured and simulated maximum

realized gain versus frequency plot of the sample with and without metamaterial. From the figure it is clearly indicative that a sharp fall of gain to -10 dBi at notch frequency 5.63 GHz whereas the gain ranges from 2 to 6.45 dBi in the rest of the UWB spectrum with metasurface. Fig .6(a),(b) show the simulated and measured E- and H-plane radiation pattern at 4GHz, 6.5GHz and 8.5GHz respectively .E-plane radiation pattern with axial null along the axis of the antenna (y-axis) was obtained which is E-plane monopole type of pattern and almost omni-directional H-plane pattern was obtained. The frequencies are chosen over the UWB spectrum except the notch frequency due to non radiative mode of antenna at notch.

B. Dual Notched Metamaterial Loaded Antenna

Housing two spur lines with different length (l_{vs1} =12.85 mm and l_{vs2} = 9.98 mm) on the feeding microstrip line of the monopole, results in dual notched UWB antenna. Fig.3(c) and (d) show the photograph of the fabricated dual notched UWB antenna without and with meta-surface respectively. Fig.7 shows simulated and measured S_{11} versus frequency plot of this antenna with and without metamaterial. Here, two distinct measured notches at 4.22GHz and 5.52GHZ are observed contributed by two spur against 4.10 GHz and 5.36 GHz for simulated response. As can be revealed from the figure, the notches are quite strong (measured S_{11}= -1 dB and –2.5 dB for 1st and 2nd notches respectively) and measured S_{11} plot is in good correspondence with the simulated one. The maximum realized gain versus frequency plot of this antenna with and without metamaterial, as shown in Fig.8, also exhibits the presence of two notches contributed by the dual spur-line resonators. Measured maximum realized gain of the antenna falls to -14 dBi and -9.5 dBi at 4.22GHz and 5.52GHz while in the rest of the UWB spectrum gain ranges within (1- 5.9 dBi).Thus, as expected, the dual spur-line loaded MPA provides a satisfactory dual notched UWB performance. Fig.9 (a),(b) shows the simulated and measured E-plane and H-plane radiation pattern of this antenna at 3.5 GHz , 6.5 GHz and 8.5 GHz respectively .Like the previous case of single notched UWB antenna, here also antenna provides monopole type radiation pattern with directional E-plane and nearly omni-directional H-plane pattern. Consequently the projected method of multiple spur-line embedded on the feed part of the antenna does not have noteworthy impact on the radiation performance of the antenna over the entire UWB band apart from the notch frequencies.

C. Triple Notched Metamaterial Loaded Antenna

To establish the triple notched UWB performance, as shown in Fig.3(e),(f) a third spur line is housed on the microstrip feed line. Fig.10 shows the simulated and measured S11 of the triple notched UWB antenna with and without metamaterial. Like the previous configurations, the quarter wave spur-line contributes three measured notch frequencies at 4.63 GHz ,5.75 GHz and 7.72 GHz compared to 4.52GHz , 5.61 GHz and 7.62 GHz obtained in full wave analysis .The maximum realized gain of the antenna also reveals the presence of these notches with significantly reduced gain of -10.5 dBi,-11.5 dBi and -14.5 dBi at measured notch frequencies as shown in fig.11 . As shown in simulated and measured radiation pattern of Fig.12, the triple notched antenna contributes to good omni-directional pattern over the entire UWB spectrum.

Table1: Design parameters of Square shaped Metamaterial implanted ultra wideband antenna with multi frequency notched characteristics

Antenna parameters	mm
L	50
W	50
h	1.575
L_G	21.5
R	12.5
w_m	5
Spur line 1: (i=1) l_{hs1}	0.68
l_{vs1}	9.67
Spur line 2:(i=1,2) l_{hs1}	1.32
l_{vs1}	12.85
l_{hs2}	0.5
l_{vs2}	9.98
Spur line 3: (i=1,2,3) l_{hs1}	0.7
l_{vs1}	12
l_{hs2}	1.42
l_{vs2}	9
l_{hs3}	0.6
l_{vs3}	7.13
Metamaterial dimension : h_i X l_i	2X2

Table 2: Notched frequencies of Square shaped Metamaterial implanted ultra wideband antenna with spur line resonator for three different configuration

Configuration		Obtained Notch Frequency		
		Computed	Simulated	Measured
Single spur line loaded monopole	f_{n1}	5.52	5.53	5.63
Dual spur line loaded monopole	f_{n1}	4.16	4.10	4.22
	f_{n2}	5.35	5.36	5.52
Triple spur line loaded monopole	f_{n1}	4.45	4.52	4.63
	f_{n2}	5.59	5.61	5.75
	f_{n3}	7.32	7.62	7.72

A comparative table is shown in table 3.From the table it is clear that due to square shaped meta material the gain of the antenna significantly improved.

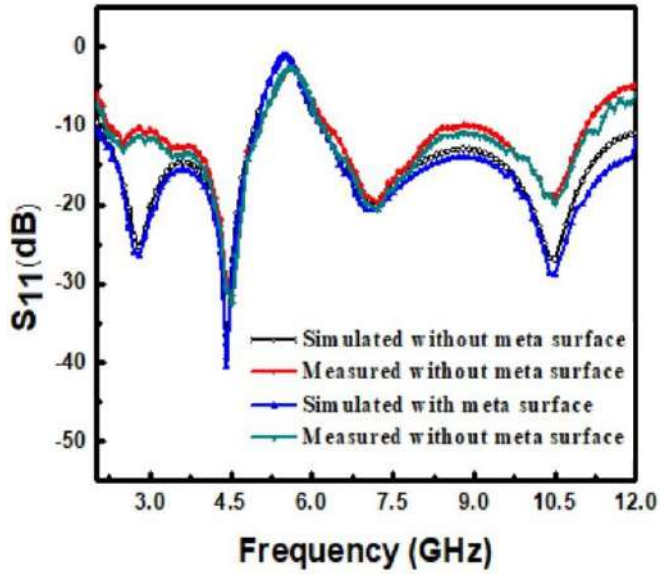

Fig.4. Simulated and measured S_{11} characteristics with and without metamaterial for single notch.

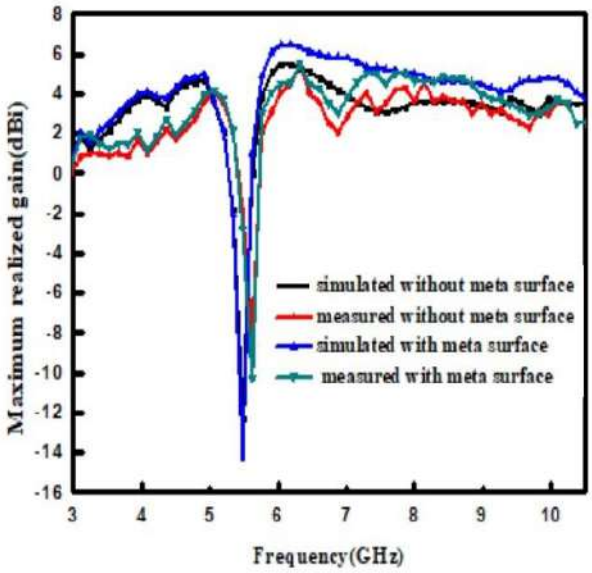

Fig.5. Maximum realized gain of the proposed single-notched microstrip fed circular monopole antenna with and without metamaterial.

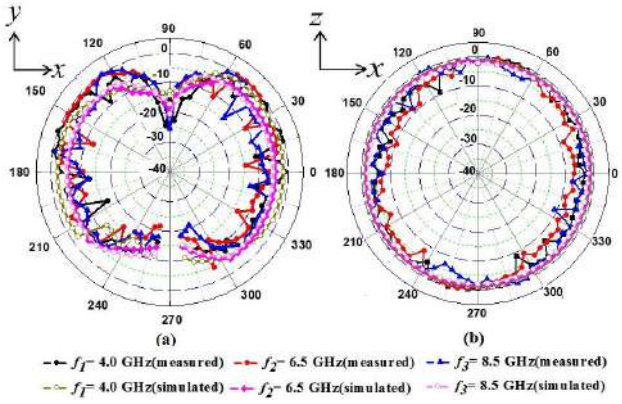

Fig.6. Simulated and measured normalized (a) E (X-Y) and (b) H (X-Z) plane co-pole radiation pattern at various frequencies with metamaterial for single notch.

INTERNATIONAL JOURNAL OF MICROWAVE AND OPTICAL TECHNOLOGY,
VOL.18, NO.3, MAY 2023

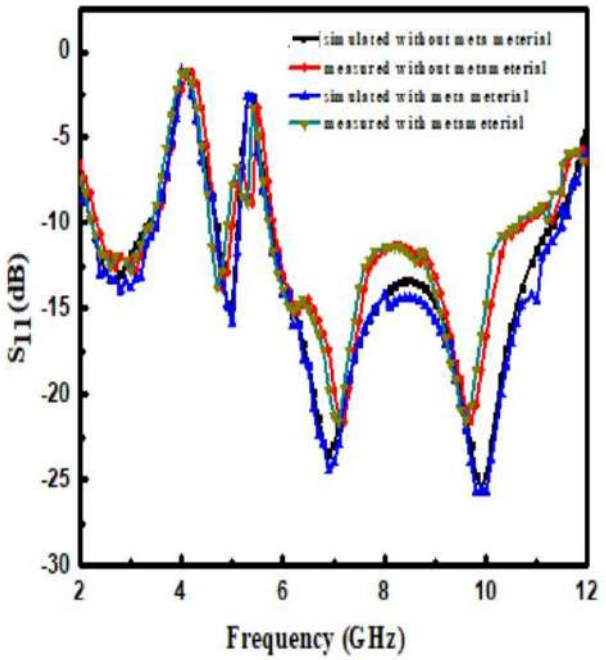

Fig.7. Simulated and measured S_{11} characteristics with and without metamaterial for dual notch.

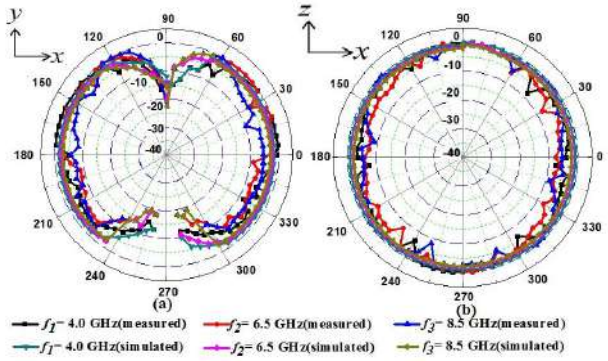

Fig.9. Simulated and measured normalized (a) E (X-Y) and (b) H (X-Z) plane co-pole radiation pattern at various frequencies with metamaterial for dual notch.

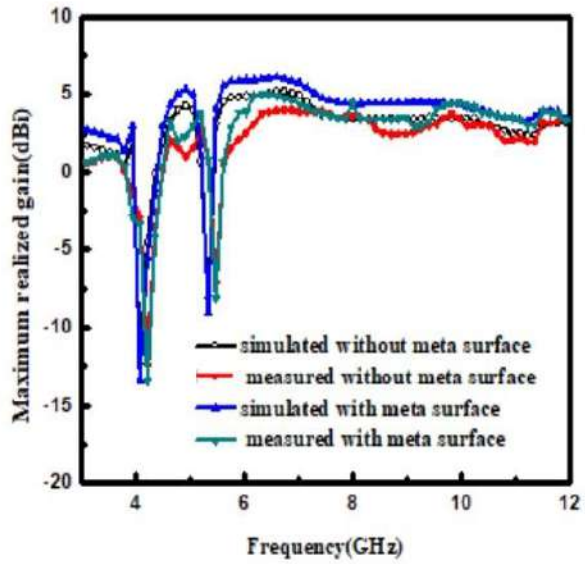

Fig.8. Maximum realized gain of the proposed double-notched microstrip fed circular monopole antenna with and without metamaterial.

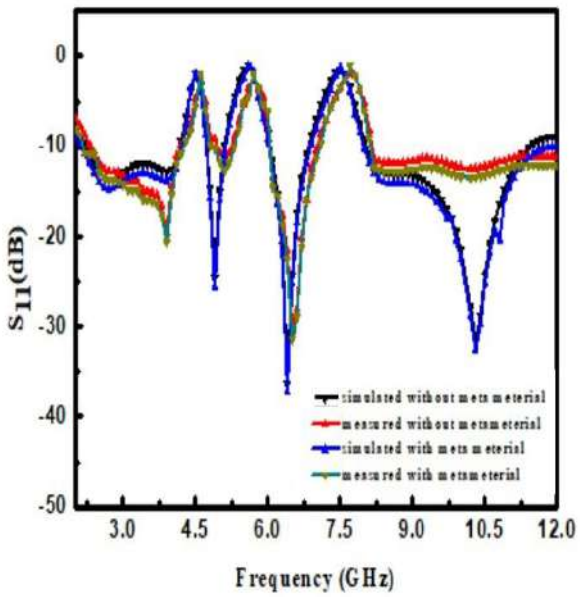

Fig.10. Simulated and measured S_{11} characteristics with and without metamaterial for triple notch.

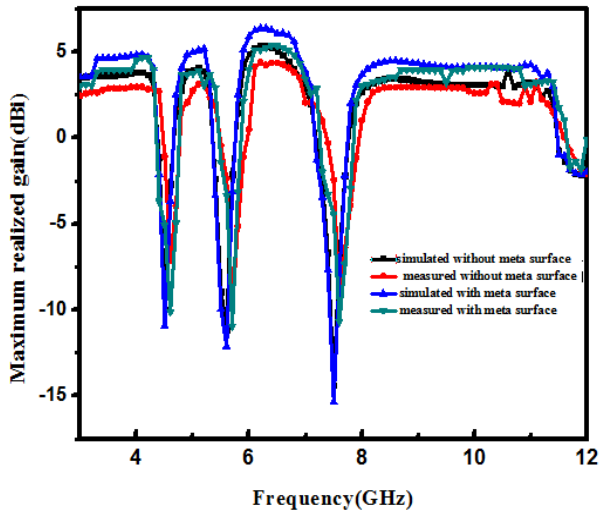

Fig.11. Maximum realized gain of the proposed triple-notched microstrip fed circular monopole antenna with and without metamaterial.

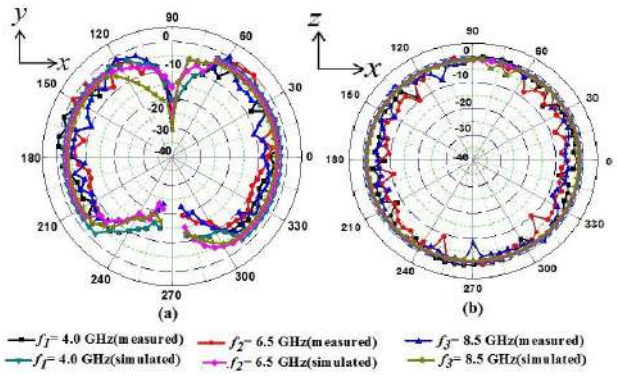

Fig.12. Simulated and measured normalized (a) E (X-Y) and (b) H (X-Z) plane co-pole radiation pattern at various frequencies with metamaterial for triple notch.

Table3: Comparison of Metamaterial Implanted Ultra wideband Monopole Antenna with other Monopole structure

References	Size (LXW) mm^2	Band width (GHz)	Notch frequency (GHz)	Return loss (dB)	Maximum Gain (dBi)
[3]	40X40	8.37	5.56	-30	-
[5]	54X47	8.0	2.4,3.5,5.8	-28 -29 -40	2 -4.5
[6]	20X18	9.0	3.7 5.7	-25	3.5-5.5
[7]	18X15	10.9	5.7	-30	2.5-5.5
[9]	50X50	8.0	3.7 ,5.6	-45	2-3.5
Proposed	50X50	10.0	5.53 4.10,5.36 4.52,5.61, 7.62	-25 -40 -40	3 - 6.45

IV. CONCLUSION

In this paper, a very easy but exceptionally proficient design of improved frequency notched UWB metamaterial loaded antenna is presented. Accommodating single/multiple quarter wavelength spur-lines on the feeding microstrip excites spur's resonance which in turn contributes to the frequency notch/notches in the UWB antenna. A widely known circular ultra wide band monopole antenna is preferred to exhibit notch characteristics. Design concept is verified in a comprehensive manner with systematic investigation using 3-D full wave simulation and impedance and radiation characteristics of the entire fabricated prototype. By loading these antennas with square shaped metasurface, there is little bit improvement of gain of the antenna. Improvement of antenna performance using square shaped meta-surface is the novelty of the design.

REFERENCES

[1] Buchwald, Z. 'The Creation of Scientific Effects: Heinrich Hertz and Electric Waves'. *The University of Chicago Press*, September, 1994.

[2] FCC, 'Report of the spectrum efficiency working group', November,2002, (*FCC Spectrum Policy Task Force, Tech. Rep*., 2002)

[3] Xinan Qu, Shun-Shi Zhong, Wei Wang, 'Study of the band-notch function for a UWB circular disc monopole antenna', *Microwave and Optical Technology Letters*, vol. 48, no. 8, pp. 1667– 1670, August 2006.

[4] Salman Naeem Khan, Jiang Xiong, Sailing He, 'Low profile and small size frequency notched planar monopole antenna from 3.5 to 23.64 GHz', *Microwave and Optical Technology Letters*, vol. 50, no.1, pp. 235– 236, January 2008.

[5] Yan Zhang, Wei Hong, Chen Yu, Zhen-Qi Kuai, Yu-Dan Don, Jian-Yi Zhou, " Planar Ultrawideband antennas with multiple notched bands based on etched slots on the patch and/or split ring resonators on the feed line", *IEEE Transactions on Antennas and Propagation*, vol. 56, no. 9, pp. 3063–3068, September 2008.

[6] M.Abdollahv and, G. Dadashzadeh, D. Mostafa, "Compact dual band-notched printed monopole antenna for UWB application", *IEEE Transactions on Antennas and Propagation*, vol. 9, pp. 1148–1151, December 2010.

[7] A. Nouri, G. R. Dadashzadeh, "A compact UWB band-notched printed monopole antenna with defected ground structure*", IEEE Transactions on Antennas and Propagation*, vol. 10, pp. 1178–1181, October 2011.

[8] James R. Kelly, Peter S. Hall, Peter Gardner, "Band-notched UWB antenna incorporating a microstrip open-loop resonator", *IEEE Transactions on Antennas and Propagation*, vol. 59, no. 8, pp. 3045–3048, August 2011.

[9] Jawad Yaseen Siddiqui, Chinmoy Saha, Yahia M. M. Antar, "Compact SRR loaded UWB circular monopole antenna with frequency notch characteristics", *IEEE Transactions on Antennas and Propagation*, vol. 62, no. 8, pp. 4015–4020, Aug. 2014.

[10] M. Barbuto , F. Bilotti and A. Toscano "SRR-based Notch Filter for Horn Antennas", *8th International Congress on Advanced Electromagnetic Materials in Microwaves and Optics – Metamaterials 2014* Copenhagen, Denmark, pp 46-48 August 2014

[11] Jawad Y. Siddiqui, Chinmoy Saha, Chittajit Sarkar, Latheef A. Shaik, and Y.M. M. Antar "Ultra-Wideband Antipodal Tapered Slot Antenna With Integrated Frequency Notch Characteristics" *IEEE Transactions on Antennas and Propagation*, vol. 66, no. 3, pp. 1534-1539, March 2018.

[12] SCHIFFMAN, B. M., MATTHAEI, G. L. "Exact design of bandstop microwave filters", *IEEE Transactions on Microwave Theory and Techniques*, pp. 6-15, Jan. 1964.

[13] BATES, R. N. "Design of microstrip spur line bandstop filters", *IEEE Journal on Microwave Optics and Acoustics*, vol. 1, no. 6, pp. 209-214, Nov. 1977.

[14] NGUYEN, C., HSIEH, C., BALL, D.W. "Millimeter wave printed circuit spur line filter" , *IEEE MTT-S International Microwave Symposium Digest*, pp. 98-10, 1983.

[15] Liu H, Sun L and Shi Z, "Dual Bandgap Characteristics of Spurline Filters and its Circuit Modeling" , *Microwave and Optical Technology Letters* , 49, 2805-2807,2007.

[16] Haiwen Liu, Rui Cao, Manqing Wu. "Harmonics suppression of Wilkinson power divider using spur lines with adjustable rejection bands" . *IEEE MTT-S International Microwave Symposium Digest*, vol. 1, pp. 189-192, 2008.

[17] Chong Cheaw Chamnan , Shafique, M. Robertson, I. D. "Miniaturization and electronic tuning techniques for microstrip spurline filters", *IET Microwaves, Antennas & Propagation*, vol. 5, pp. 1-9, 2011.

[18] Yoonjae Lee, Ganguly, S. and Mittra, R., "Multi-band L5-capable GPS antenna with reduced backlobes", *IEEE International Symposium on Antennas and Propagation*, vol. 1A, pp. 3-8, July,2005.

[19] J. Liang, L. Guo, C. C. Chiau, X. Chen, and C. G. Parini, "Study of a Printed Circular Disc Monopole Antenna for UWB Systems" *IEEE Transactions on Antennas and Propagation*, vol. 53, no. 11, pp. 3500-3504, Nov.2005.

[20] J. Liang, L. Guo, C. C. Chiau, X. Chen, and C. G. Parini, "Study of CPW-fed circular disc monopole antenna for ultra wide band applications," *IEE Proc. Microw. Antennas Propagat*., vol. 152, no. 6, pp.520–526, Dec. 2005.

[21] I. Bahl and P. Bhartia, *Microwave Solid State Circuit Design*, Hoboken, NJ, USA: Wiley, 1998, ch. 2.

[22] High Frequency Simulation Software, Ansoft Corp., vol. 14.

Null Placement in Uniform Linear Array by Phase Control of Edge Elements

Sandipan Mitra[1], Soumyo Chatterjee[2], Sayan Chatterjee[3]

[1]Dept. of ECE, Institute of Engineering and Management, Kolkata-700091, India
[2]Dept. of ECE, Heritage Institute of Technology, Kolkata-700107, India
[3]Dept. of ETCE, Jadavpur University, Kolkata-700032, India
e-mail: (sandipanmitra97@gmail.com, soumyo.chatterjee@heritageit.edu and sayan1234@gmail.com)

Abstract.

This paper presents a novel method of null placement by controlling only the excitation phase of the edge elements of a uniformly excited linear antenna array. Antenna parameters such as directivity, First Null Beam Width (FNBW) and Half Power Beam Width (HPBW) are obtained analytically through array synthesis. Then the pattern gets degraded due to the required null placement. Subsequently to enhance the pattern, antenna parameters and to find out the optimum value of the excitation phase, suitable evolutionary algorithm has been employed. The whole simulation is carried out using a 10-element uniform, linear antenna array by two different approaches to comparatively study the effects.

Keywords. Null placement, Phase control, Edge element, Array symmetric method, Classical DE algorithm

INTRODUCTION

In the modern era of communication system, a major role is played by antenna. Starting from Wi-Fi, Bluetooth, GPS, etc. to RADAR, SONAR, UAVs to Satellite Communications, every single wireless gadget requires an antenna and more specifically an antenna array [1]. But the objective of an antenna is not restricted to just transmitting and receiving signals, it should also be able to optimize radiated energy in some particular required direction and should be able to suppress it in other directions. Although the antenna directivity can be increased by increasing the number of array elements or by reducing the inter element spacing [2] but still suppression of unwanted signals is very essential for further increase in directivity. Generally, this suppression of unwanted signals is done by masking the interference signal from a particular direction. This method of masking is known as null placement and in earlier times researchers used to place nulls analytically [3-6], but later researchers found out that due to this analytical placement of null, various antenna parameters are deteriorating and moreover multiple null and wide null cannot be placed analytically. This gave rise to the use of evolutionary algorithms to overcome the limitations.

V2X Communication Challenges and Performance Evaluations for Cooperative Multi-hop Platooning

Nidhi C. Vasa, Annesha Das Sarma, Aniket Hait, Prasad Ranjan Deb and Ananya Chattopadhyay
ECE Department, Heritage Institute of Technology, Kolkata, India.
Corresponding Author: ananya.chattopadhyay@heritageit.edu

***Abstract*—To enable widespread large-scale automotive network access, traditional vehicle-to-everything (V2X) technologies are evolving to the Internet of Vehicles (IoV) where the vehicles are becoming smart with the aid of booming technologies improving the driving experience. In order to address the increasing demands on emerging advanced vehicular applications, such as intelligent transportation systems (ITS) and autonomous vehicles, the use of 5th Generation (5G) millimeter wave (mmWave) frequencies ate the efficient choice. While mmWave communications will enable massive data rates and low latency, the propagation characteristics become very challenging for accurate performance evaluations under V2X scenarios. We investigate the impact of different propagation scenarios and system parameters, including the inter-vehicle distance for platooning in highways. We have considered the blockage by other vehicles in busy traffic roads and multi-hop relayed vehicle-to-vehicle (V2V) communication and provide guidelines towards the most promising V2V deployment configurations.**

Index Terms - Millimeter wave, busy traffic, blockage, road side unit, antenna height, data rate.

1. Introduction

The rapid evolution towards 5th generation (5G) wireless networks will accelerate the developments of Connected Intelligent Transportation Systems (C-ITSs) to deliver improved traffic safety and efficiency through autonomous driving [1]. In this era, millimeter wave (mmWave) communications became obvious choice for modern vehicular networks because of it's widespread frequency range and enormous bandwidth capacity. For commercialized C-ITSs use cases, the capacity requirements are over exceeded than current communication technologies for vehicular networks [2]. For advanced safety applications in cooperative multi-hop platooning, the vehicles exchange processed sensor data to improve the coverage and accuracy of environmental perceptions. Moreover, for high degree of automation, the system latency must be very small to ensure prompt reactions to unpredictable events. In all such scenarios, the system data rate requirements can be approximately 1-10 Gbps for high-quality uncompressed images [3].

Vehicle to Everything (V2X) is a vehicular communication system that helps in transferring the information from a vehicle to any moving parts of a traffic system that can affect the vehicle by any means [4]. It incorporates some specific applications (shown in Figure 1) such as, (i) Vehicle to Infrastructure (V2I) - refers to techniques for connecting cars with road management systems, (ii) Vehicle to Vehicle Communication (V2V) - implies a future in which cars, vans, trucks and even motor bikes will communicate directly with each other, (iii) Vehicle to Network Communication (V2N) - enables access to in-vehicle service providers and infotainment streams, (iv) Vehicle to Cloud Communication (V2C) - leverages V2N access to broadband cellular mobile networks to offer data exchange with the cloud, (v) Vehicle to People Communication (V2P) - establishes a direct communication between a vehicle and a pedestrian and (vi) Vehicle to Grid Communication (V2G) - provides bidirectional data exchange between plug-in hybrid vehicles, battery electric vehicles and even hydrogen fuel cell vehicles with the smart grid in support of electrification of transport.

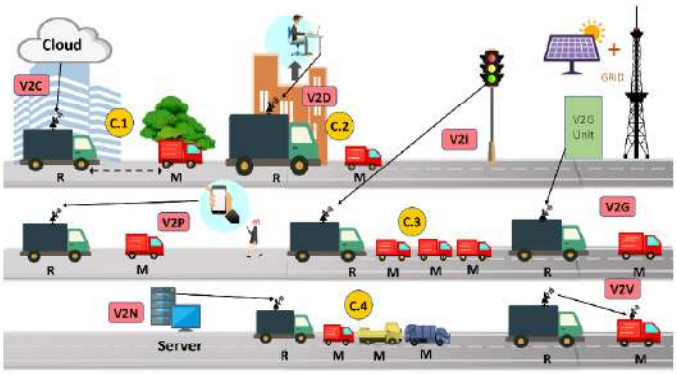

Fig. 1. Applications and Challenges of V2X Communication

In the world of ITS for autonomous vehicles, platooning or flocking is a method for driving a group of vehicles together to increase the capacity of roads via an automated highway system. Platooning may be either maned vehicle or fully automatic unmanned vehicle or hybrid. By exchanging information among vehicles through communication networks, vehicle platooning can significantly improve traffic safety and efficiency. Modern communication such as Bluetooth and wireless, GPS, radar-sensing systems plus drive-by-wire steering and throttle allows for computers to take control of cars.

There are many designing issues and challenges for V2X platooning (shown in Figure 1) listed below:

1) If the gap between two platooning vehicles is larger

Tuning of Fuzzy Controller by Variable Clustered Fuzzy Rules and Its Application to Overhead Crane

Authors Indrajit Naskar, AK Pal, Nandan Kumar Jana

Publication date 2023/1/27

Conference 2023 International Conference on Intelligent and Innovative Technologies in Computing, Electrical and Electronics (IITCEE)

Pages 119-124

Publisher IEEE

Description This paper proposed efficient rule extraction and rule reduction methods for the self-tuning fuzzy controller. The Fuzzy Clustering Method (FCM) and similarity approach are applied to extract and reduce the fuzzy gain rules. The proposed rule extraction scheme is investigated on a self-tuning fuzzy proportional plus derivative controller (STFLPDC), having 49 fuzzy rules and 49 fuzzy gain rules. The utility of the scheme is validated with various clustering validity indices. The effectiveness of the self-tuning fuzzy controller with the different reduced number of extracted fuzzy gain rules generated from clustering data is found to be quite satisfactory in comparison with the initial (49) fuzzy gain rules. The effect of gain rule variations on STFLPDC is tested to control the position and swing of an overhead crane and a comparison is made with other fuzzy and conventional controllers.

CHAPTER 20

APPLICATION OF EFFICIENT MOVING LEAST SQUARES METHOD ON ROBUST DESIGN OPTIMIZATION

TUSHAR DAS[1] and SOUMYA BHATTACHARJYA[2]

[1]Assistant Professor, Department of Civil Engineering, Heritage Institute of Technology, Kolkata, West Bengal, India

[2]Associate Professor, Department of Civil Engineering, Indian Institute of Engineering Science and Technology, Shibpur, West Bengal, India, E-mail: soumya@civil.iiests.ac.in

ABSTRACT

The engineering community has recognized that structural optimization not considering uncertainty will result in catastrophic failure consequences. Often, such failures cause the loss of many lives. Thus, this issue is attempted by the researchers by exploring various approaches to optimization under uncertainty. Among these, Robust Design Optimization (RDO) is the most popular one, which ensures reliability as well as the least deviation of structural performance under uncertainty. One of the conventional ways of accomplishing RDO is to apply Monte Carlo Simulation (MCS), which is associated with large computational time. Often, surrogate-assisted optimization schemes are adopted to circumvent this computational challenge. But such approaches are hinged on the conventional least squares method, which is often observed to be a source of error in the existing literature. Thus, the issues of either enormous error

Optimization Methods for Engineering Problems. Dilbagh Panchal, Prasenjit Chatterjee, Mohit Tyagi, Ravi Pratap Singh (Eds.)

IEEE 802.11ac vs 802.11ad for V2X: How Many Frames Can We Aggregate?

Ananya Chattopadhyay* and Aniruddha Chandra†
*ECE Department, Heritage Institute of Technology, Kolkata 700107, WB, India
†ECE Department, National Institute of Technology, Durgapur 713209, WB, India
Email: ananya.chattopadhyay@heritageit.edu, aniruddha.chandra@ieee.org

***Abstract*—Despite the high relative velocity, the coherence time in vehicle-to-everything (V2X) multipath fading channel does not linearly decrease with the increase in frequency or velocity, especially when directional propagation or beamforming is involved. Therefore, multiple data frames can be aggregated spanning a coherence time slot. Aggregation of data frames helps to avoid channel estimation after each frame transmission and contributes towards efficient utilization of bandwidth through reduction of protocol overhead. This ultimately leads to enhancement of throughput and data rate in vehicular environment. In this paper, we have addressed two types of frame aggregation, first, aggregated MAC service data unit (A-MSDU), where the medium access control (MAC) layer receives aggregated frames from the upper layers, and second, aggregated MAC protocol data unit (A-MPDU), where the MAC layer frames are aggregated and are send to physical (PHY) layer. Both these frame aggregation strategies are studied in the context of vehicle-to-infrastructure (V2I) and vehicle-to-vehicle (V2V) communications. Our ultimate goal is to compare network performance of IEEE 802.11ac and 802.11ad standards with different types of frame aggregation in V2I and V2V scenarios. IEEE 802.11ac and 802.11ad are the amendments to IEEE 802.11 and are possible candidates for realizing a multi-gigabit V2X wireless system, to satisfy emerging bandwidth hungry applications such as autonomous driving. We observed that frame aggregation is more effective in IEEE 802.11ac compared to 802.11ad. Also, in general, more aggregations are possible with A-MSDU than with A-MPDU. Further, the allowable number of frames to be aggregated for V2V is an order higher than V2I irrespective of the type of aggregation or standard, and higher aggregations are achieved in the lower range of beamwidth, velocity or frequency.**

***Index Terms*—Vehicular Communication, Channel Coherence Time, Directional Beamwidth, IEEE Standards, Frame Aggregation.**

I. Introduction

With the advancement of fifth generation (5G) systems, we are on the brink of a new era for the vehicular wireless communication, which imposes new challenges for designing potential roadmap [1]. In recent years, vehicle-to-vehicle (V2V) and vehicle-to-infrastructure (V2I) communications, which are collectively named as vehicle-to-everything (V2X) communications, have been successfully applied in automotive industry for safety signaling information, high definition video surveillance, passengers Internet access services, etc. [2]. To support seamless connectivity on move, IEEE 802.11ac and 802.11ad, the two popular amendments of IEEE 802.11, are used through multi-gigabit wireless system (MGWS) by integrating different technologies, intelligence, and flexibility. A large amount of data are generated and exchanged for any moving vehicle to get an accurate perception of their surrounding environment with nearby Road Side Unit (RSU) or neighboring vehicles. This, in turn, increases the system overhead.

To deal with the numerous communication overhead, frame aggregation is the most efficient way for shared channel with minimum time slot in vehicular communications. Aggregation reduces the number of channel accesses and probability of collisions in case of high contention for bursty traffic and thereby efficiently utilize the bandwidth. Both the standards, IEEE 802.11ac and 802.11ad, realize frame aggregation in two ways, aggregated MAC service data unit (A-MSDU) and aggregated MAC protocol data unit (A-MPDU).

However, there are certain limitations of frame aggregation, especially at GHz range vehicular scenario when the channel impulse response is rapidly changing with speed of the vehicle. The maximum frame size of the aggregated frame is proportional with the channel coherence time (i.e. the time for the transmission must be less than the channel coherence time). If the coherence time is low i.e. the wireless channel changes rapidly, then control information such as, the medium access, preamble and header overhead for any packet increases which provides less slot for data packet, as a result, the system data rate hampers. The directional communication in V2X with narrow beams [3] limit the spreading angle of the arrived signal, leading to smaller Doppler spread and thus larger coherence time [4], so the channel behaves quite resistant to Doppler spread even at higher speed. Therefore, optimum value for coherence time for the vehicular channel is a necessary parameter to estimate system throughput and the total number of aggregated frames for effective V2X data transmission.

The main contributions of the paper are :

- We have applied coherence time calculation given in [4] between scatterers and moving receiver into the context of directional V2I and V2V communication for large and small values of directive angle between transmitter and receiver, respectively.
- We have calculated coherence time for the variation of velocity, frequency, beamwidth and distance, and estimated the optimum value for channel coherence time for V2I and V2V communications to maximize the system throughput.
- Considering the optimum coherence time for successful data transmission, we have investigated the system perfor-

978-1-6654-8053-6/22/$31.00 ©2022 IEEE